Penkvilksite-2O: Na$_2$TiSi$_4$O$_{11}$·2H$_2$O

Marcella Cadoni[a,b] and Giovanni Ferraris[a,b]*

[a]Dipartimento di Scienze Mineralogiche e Petrologiche, Università di Torino, Via Valperga Caluso 35, 10125 Torino, Italy, and [b]Nanostructured Interfaces and Surfaces (NIS), Centre of Excellence, Via Pietro Giuria 7, 10125 Torino, Italy
Correspondence e-mail: giovanni.ferraris@unito.it

The crystal structure of synthetic penkvilksite-2O, disodium titanium tetrasilicate dihydrate, Na$_2$TiSi$_4$O$_{11}$·2H$_2$O, a microporous titanosilicate, confirms the major features of a previous model that had been obtained by order–disorder (OD) theory from the known structure of penkvilksite-1M. An important difference from the previous model involves the hydrogen bonding of the water molecule which, on the basis of a Raman spectrum and the finding of only one of the two H atoms, is proposed to be disordered about a fixed O–H direction. The structure of penkvilksite-2O is based on (100) silicate layers linked by isolated TiO$_6$ octahedra to form a heteropolyhedral framework. The layer is strongly corrugated, based on interlaced spiral chains, and is crossed by two different channels that have an effective channel width of about 3 Å.

Comment

In recent years, titanium silicates have attracted widespread attention from materials scientists because they possess properties that are useful for technological applications, *e.g.* in catalysis and ion exchange. The heteropolyhedral structure type of penkvilksite, Na$_2$TiSi$_4$O$_{11}$·2H$_2$O, which is, at the same time, layered and microporous, has been a model for the synthesis of several isotypic structures (Lin *et al.*, 1997; Liu *et al.*, 1997; Lin & Rocha, 2004, 2005, 2006). Compared with microporous monopolyhedral frameworks, like those of zeolites, the presence in the framework of higher coordination polyhedra makes the microporous heteropolyhedral structures more suitable for tuning properties *via* chemical composition [*cf.* Rocha & Lin, 2005; a recent review of microporous mineral phases is reported by Ferraris & Merlino (2005)]. Some synthetic compounds have been tested for sorption of radioactive elements (Attar & Dyer, 2001; Koudsi & Dyer, 2001) and luminescence due to the demonstrated incorporation of rare earth elements into the structure (Lin *et al.*, 2006).

Two minerals with the same ideal chemical composition Na$_2$TiSi$_4$O$_{11}$·2H$_2$O, but crystallographically different, were reported from the alkaline massifs of Lovozero and Khibiny

(Kola Peninsula, Russia) and Mont Saint-Hilaire (Canada). Merlino *et al.* (1994) showed that the Khibiny sample, first studied by them, and the Lovozero sample, used by Bussen *et al.* (1975) to define the mineral species, represent two different polytypes. These polytypes, according to Merlino *et al.* (1994), are: penkvilksite-1M (monoclinic $P2_1/c$; a = 8.956 Å, b = 8.727 Å, c = 7.387 Å and β = 112.74°) and penkvilksite-2O (orthorhombic $Pnca$; a = 16.3721 Å, b = 8.7492 Å and c = 7.4020 Å). The same authors solved the crystal structure of penkvilksite-1M from single-crystal X-ray diffraction data and, applying the order–disorder (OD) theory [Dornberger-Schiff, 1964; for a recent review of the theory, see Ferraris *et al.* (2008)], obtained a model of the structure of penkvilksite-2O and refined it by the Rietveld method using X-ray powder diffraction data obtained from a sample that also contained 5% of penkvilksite-1M. According to Merlino *et al.* (1994), penkvilksite-1M and penkvilksite-2O represent two out of four maximum degree of order (MDO) polytypes predicted by the OD theory; the other two MDO polytypes are one that is monoclinic 2M (space group $I2/c$) and another, again orthorhombic 2O, but with space group $Pmcn$. The occurrence of these further two polytypes was considered improbable
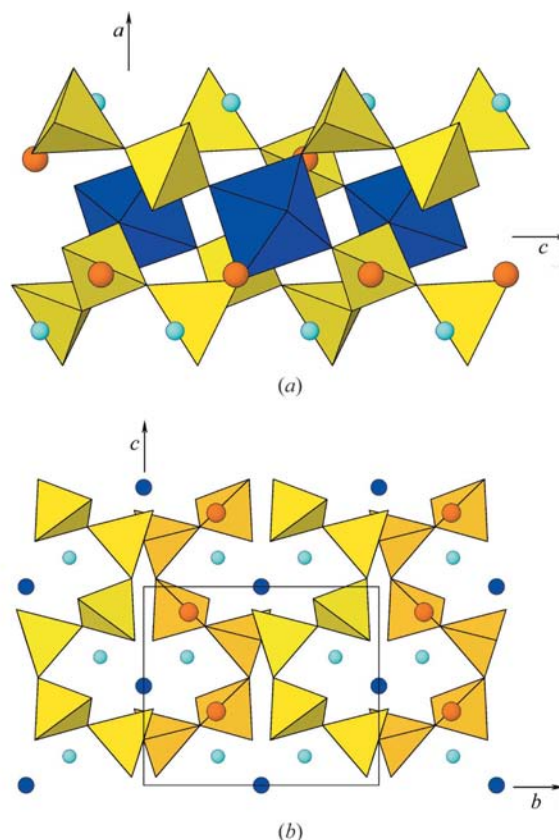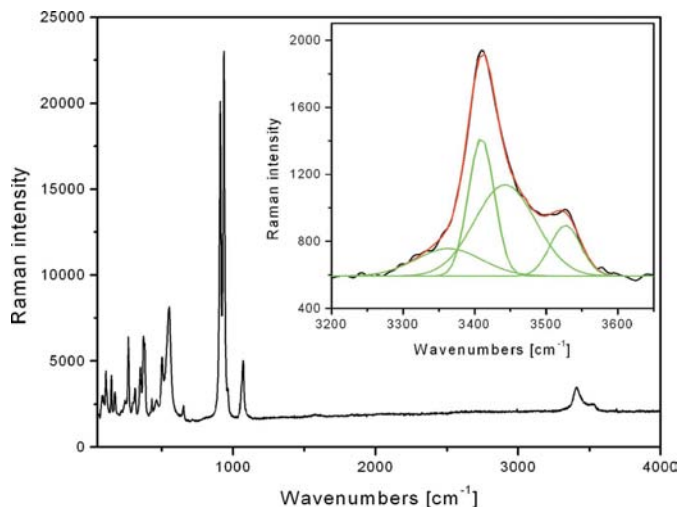

Figure 1
(*a*) A view along [010] of a module of the penkvilksite structure consisting of isolated Ti1 octahedra (dark; blue in the electronic version of the paper) and [001] chains of Si tetrahedra (light, yellow); different stackings of this module along [100] lead to the polytypes discussed in the *Comment*. (*b*) The (100) silicate layer formed by the [001] chains: clockwise and counterclockwise chains are differently coloured. Light (orange) and dark (cyan) circles represent, respectively, Na1 and water O atoms.

because the water molecules would be too close to each other, according to the structural models derived from the two known polytypes. However, Sheriff & Zhou (2004) tentatively assigned to $2M$ an unknown penkvilksite polytype found by an NMR spectroscopic study of a synthetic sample.
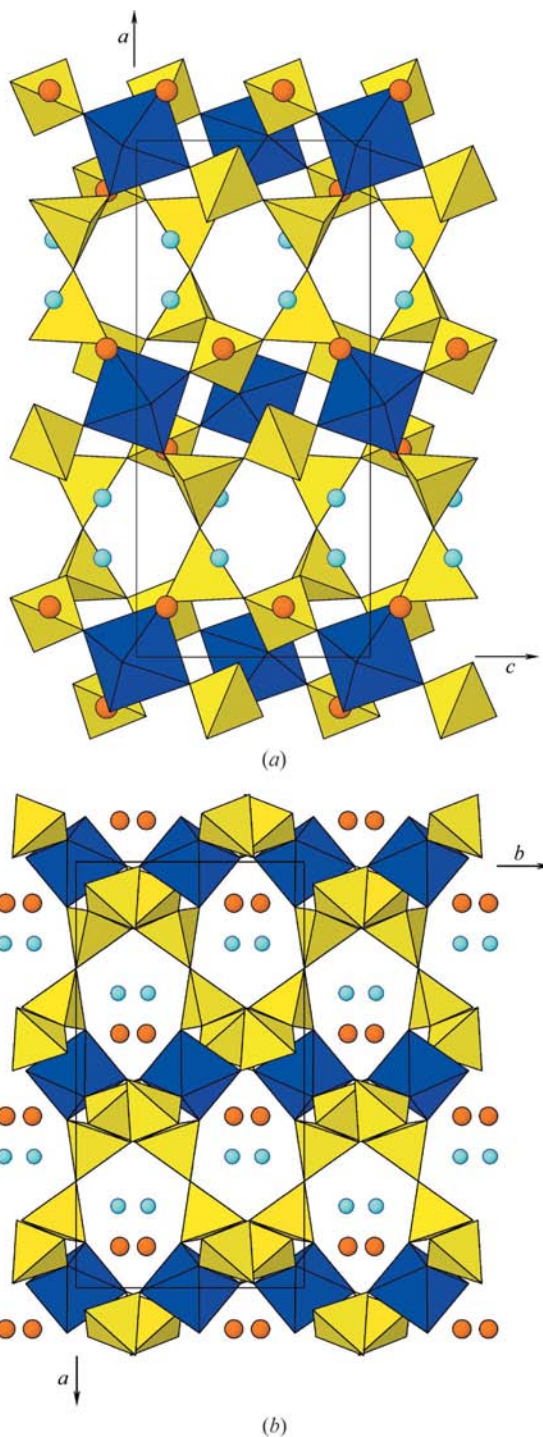
The above-mentioned MDO polytypes of penkvilksite differ only in the stacking of a basic module (Fig. 1a) with layer-group symmetry $P(1)2_1/c1$. This module is stacked by the action of the following symmetry operations: 2_1 (1M), n (2O, space group $Pnca$), 2 (2M) and m (2O, space group $Pmcn$); the MDO polytypes shown in parentheses and, in particular, silicate layers like that shown in Fig. 1b are thus formed [cf. Fig. 5 in Merlino et al. (1994)]. Both the 1M and 2O ($Pnca$) polytypes have been found several times in the syntheses of penkvilksite-type structures quoted above [1M also occurs in the mineral tumchaite, $Na_2(Zr,Sn)Si_4O_{11}\cdot 2H_2O$ (Subbotin et al., 2000)], but the crystal structure of penkvilksite-2O has not been independently determined from diffraction data. In this paper, we describe the structure of penkvilksite-2O as obtained by single-crystal X-ray diffraction data from a synthetic crystal and provide further discussion based on its Raman spectrum (Fig. 2). The most important features of the structure model obtained by OD theory are confirmed, including bond lengths and angles, in spite of the fact that the X-ray powder diffraction (XRPD) pattern used by Merlino et al. (1994) for the structure refinement contained a 5% contribution from penkvilksite-1M. However, the hydrogen-bonding scheme proposed by these authors for the water molecule must be revised taking into account details of our structural study and the Raman spectrum shown in Fig. 2.

The structure of penkvilksite-2O consists of (100) silicate layers connected by isolated TiO_6 octahedra along [100], i.e. along the stacking direction of the module shown in Fig. 1(a), such that, finally, it consists of a mixed tetrahedral–octahedral heteropolyhedral framework. The silicate layer is strongly

corrugated, being based on a spiral $Si1-Si2-Si1^{vii}-Si2^{vii}\ldots$ chain that runs along [001] and is linked to its two adjacent chains by sharing O6 (Fig. 1b; all symmetry codes correspond with those given in Tables 1 and 2). The layer is crossed by two types of channels that are delimited by six Si tetrahedra along [010] (Fig. 3a) and by six tetrahedra plus two Ti octahedra

(a)

(b)

Figure 3
Penkvilksite-2O seen (a) along [010], showing the channels delimited by Si tetrahedra (light; yellow in the electronic version of the paper) only, and (b) along [001], showing the channels delimited by Si tetrahedra and Ti1 octahedra (dark, blue). Light (orange) and dark (cyan) circles represent, respectively, Na1 and water O atoms.

Figure 2
Raman spectrum of penkvilksite-2O; the region of the O—H stretching is enlarged in the inset, showing the fitting curve (dark; red in the electronic version of the paper) that is the sum of four Gaussian curves (light, green).

along [001] (Fig. 3b). However, because of the spiral form of the silicate chains, the polyhedra delimiting the channels do not form closed rings. Consequently, the effective channel width (e.c.w.), as calculated according to McCusker *et al.* (2003) by subtracting the ionic diameter of O^{2-} (2.7 Å) from the O···O distances across each channel, can only be approximate and corresponds to about 3 Å. The channels host seven-coordinate Na1 (Table 1) and, even if they show an e.c.w. smaller than the value of 3.2 Å required to classify a structure as porous (McCusker *et al.*, 2003), allow sorption of radioactive elements (Attar & Dyer, 2001; Koudsi & Dyer, 2001), which is likely due to their open spiral development.

O7W of the water molecule establishes O···O contacts shorter than 3.1 Å, as shown in Table 2. O7W···O5 and O7W···O2^{ix} are edges of the Na1 coordination polyhedron and could not correspond to hydrogen bonds, unless the relevant O7W—H1···O angles were very bent to avoid Na1···H1 contacts. Moreover, the angle O1^{viii}···O7W··· O6^{viii} of 54.0 (1)° would require an unusually bent hydrogen bond in the case that O1^{viii} and O6^{viii} were acceptors at the same time. To propose a reasonable configuration for the water molecule, one must take into account: (i) only one residual peak in the difference electron density can be attributed to a H atom (H1); (ii) no trace of a second H atom (H′) was found; (iii) in the O—H stretching region, the Raman spectrum (Fig. 2) shows a broad structured peak (maxima at 3410 and 3527 cm^{-1}; shoulders at 3354 and 3471 cm^{-1}) that can be fitted by four Gaussian curves centred at 3363, 3409, 3422 and 3527 cm^{-1}. Reasonably, the configuration around O7W, which is twice coordinated to Na1 (Table 1) and is the donor of a medium-strength hydrogen bond to O1^{viii}, can be represented as follows. Due to the unfavourable geometry required to establish an O7W—H′···O6^{viii} hydrogen bond, the O7W—H′ direction is disordered (likely by rotation around O7W—H1) and may alternatively establish very bent hydrogen bonds with O2^{ix}, O5 and O6^{viii}. Note that, despite

Figure 4
SEM image showing (100) tabular crystals of synthetic penkvilksite-2O.

the fact that O7W···O2^{ix} and O7W···O5 correspond to edges of the Na1 coordination polyhedron, the O1^{viii}···O7W···O5 and O1^{viii}···O7W···O2^{ix} angles (Table 2) actually match the range of values expected for an acceptor–donor–acceptor angle of bent hydrogen bonds (*cf.* Chiari & Ferraris, 1982). In conclusion, the maxima given above for the four Gaussian curves fitting the O—H stretching range of the Raman spectrum (Fig. 2) should correspond, in the order from lower to higher frequencies, to hydrogen bonds O7W—H′···O5, O7W—H1···O1^{viii}, O7W—H′···O6^{viii} and O7W—H′···O2^{ix}. In particular, the sharpest fitting peak at 3410 cm^{-1} is originated by the ordered O7W—H1···O1^{viii} hydrogen bond, whereas the three statistically disordered O7W—H′···O hydrogen bonds contribute to the features of the Raman spectrum shown in the inset of Fig. 2.

In conclusion, our single-crystal diffraction and Raman study improves – particularly for the description of hydrogen bonding and the microporous structure – the structural characterization of penkvilksite-2O, whose structure type was shown in several reports to be technologically important for its exchange and photoluminescent properties. At the same time, aside from details of the hydrogen bonding, the present results confirm the structure model deduced from OD theory (Merlino *et al.*, 1994), thus providing a further example of the power of this theory in modelling unknown polytypes (*cf.* Ferraris *et al.*, 2008).

Experimental

Crystals of penkvilksite-2O (Fig. 4) were obtained as a product of hydrothermal runs directed at the synthesis of rhodesite-type microporous silicates (*cf.* Ferraris & Gula, 2005) using a mixture with composition $1.10SiO_2$:$0.065TiO_2$:$0.220SrO$:$0.725Na_2O$:$0.20K_2O$. A gel with this composition was prepared by adding solutions of titanium isopropoxide in ethanol and, subsequently, of strontium nitrate, under vigorous stirring, to a strongly alkaline gel obtained by dissolving fumed silica in NaOH and KOH solution. Static crystallization was carried out in a 25 ml Teflon-lined stainless steel autoclave at 503 K, under autogenous pressure, for a period of 12 d.

An X-ray powder diffraction pattern collected on a Siemens D5000 diffractometer using Cu $K\alpha$ radiation revealed the presence of quite pure penkvilksite-2O with minor ETS-4 (Engelhard titanosilicate number 4; Rocha & Anderson, 2000). Examination by scanning electron microscopy (SEM; Stereoscan S360 Cambridge electron microscope equipped with an Energy 200 Oxford Instruments EDS apparatus) was carried out and a secondary electron image of (100) tabular penkvilksite-2O is shown in Fig. 4. The Raman spectrum reported in Fig. 2 was collected using a LabRam HR800 micro-Raman spectrometer (Jobin Yvon, equipped with a HeNe laser at an excitation wavelength of 562 nm, a CCD detector and an Olympus BX41 optical microscope).

Crystal data

$Na_2TiSi_4O_{11}\cdot2H_2O$	$V = 1053.2$ (2) Å^3
$M_r = 418.10$	$Z = 4$
Orthorhombic, *Pnca*	Mo $K\alpha$ radiation
$a = 16.320$ (2) Å	$\mu = 1.43$ mm^{-1}
$b = 8.7378$ (9) Å	$T = 295$ (2) K
$c = 7.3854$ (8) Å	$0.10 \times 0.09 \times 0.02$ mm
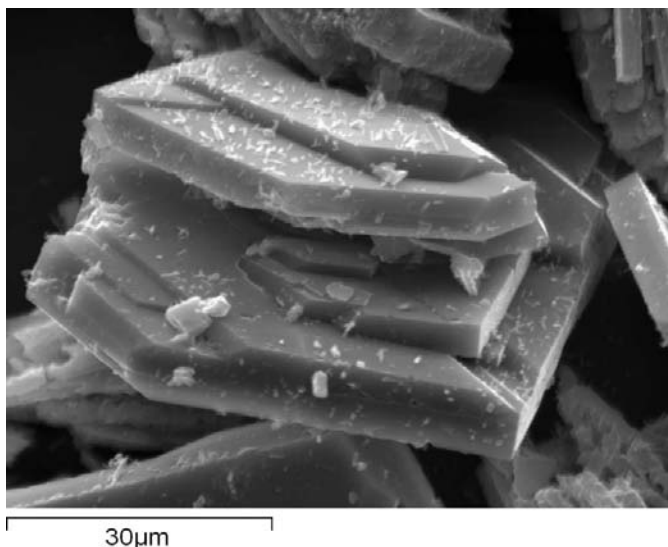
inorganic compounds

Data collection

Bruker SMART APEX diffractometer	13075 measured reflections
Absorption correction: multi-scan (*SADABS*; Sheldrick, 2002)	1306 independent reflections
$T_{min} = 0.871$, $T_{max} = 0.972$	1109 reflections with $I > 2\sigma(I)$
	$R_{int} = 0.082$

Refinement

$R[F^2 > 2\sigma(F^2)] = 0.076$	94 parameters
$wR(F^2) = 0.161$	H-atom parameters not refined
$S = 1.23$	$\Delta\rho_{max} = 1.13$ e Å^{-3}
1306 reflections	$\Delta\rho_{min} = -1.13$ e Å^{-3}

Table 1
Selected bond lengths (Å) for penkvilksite-2*O*.

Si1—O2	1.601 (4)	Si2—O6	1.606 (2)
Si1—O3	1.614 (4)	Si2—O5	1.611 (5)
Si1—O4	1.645 (4)	Si2—O4^{vii}	1.622 (4)
Si1—O1	1.647 (5)	Si2—O1	1.641 (5)
Ti1—O2^{i}	1.911 (4)	Na1—O7W^{iv}	2.273 (7)
Ti1—O5	1.964 (4)	Na1—O5^{v}	2.348 (5)
Ti1—O3	1.986 (4)	Na1—O3^{ii}	2.361 (5)
Na1—O2^{vii}	2.389 (5)	Na1—O7W^{v}	2.764 (8)
Na1—O4^{vii}	2.480 (5)	Na1—O3^{vi}	2.892 (6)

Symmetry codes: (i) $x, \frac{1}{2} - y, -\frac{1}{2} + z$; (ii) $-x, \frac{1}{2} + y, \frac{1}{2} - z$; (iv) $x, y, 1 + z$; (v) $x, \frac{3}{2} - y, \frac{1}{2} + z$; (vi) $-x, 1 - y, 1 - z$; (vii) $x, \frac{1}{2} - y, \frac{1}{2} + z$.

Table 2
Contact distances (Å) and angles (°) involving the water molecule.

O7W···O5	2.685 (7)	O7W—H1	1.10
O7W···O1^{viii}	2.788 (7)	H1—O1^{viii}	1.78
O7W···O6^{viii}	2.985 (6)	O7W···O2^{ix}	3.053 (8)
O7W—H1···O1^{viii}	150	O1^{viii}···O7W···O2^{ix}	136.6 (3)
O1^{viii}···O7W···O5	149.4 (3)	O1^{viii}···O7W···O6^{viii}	54.0 (1)

Symmetry codes: (viii) $-x + \frac{1}{2}, \frac{1}{2} + y, z - \frac{1}{2}$; (ix) $x, -y + \frac{1}{2}, z - \frac{1}{2}$.

Only one H atom is reported for the water molecule because the second one is disordered, as discussed in the *Comment*. The coordinates of this atom are derived from the difference electron density map and were not refined.

Data collection: *SMART* (Bruker, 2004); cell refinement: *SMART*; data reduction: *SAINT-Plus* (Bruker, 2004) and *SADABS* (Sheldrick, 2002); program(s) used to solve structure: *SHELXS97* (Sheldrick, 2008); program(s) used to refine structure: *SHELXL97* (Sheldrick, 2008); molecular graphics: *ATOMS* (Dowty, 2002); software used to prepare material for publication: *SHELXL97*.

References

Attar, L. A. & Dyer, A. (2001). *J. Radioanal. Nucl. Chem.* **247**, 121–128.
Bruker (2004). *SMART* (Version 5.628) and *SAINT-Plus* (Version 6.45a). Bruker AXS Inc., Madison, Wisconsin, USA.
Bussen, I. V., Men'shikov, Yu. P., Mer'kov, A. N., Nedorezova, A. P., Uspenskaya, Ye. I. & Khomyakov, A. P. (1975). *Dokl. Earth Sci.* **217**, 126–129.
Chiari, G. & Ferraris, G. (1982). *Acta Cryst.* B**38**, 2331–2341.
Dornberger-Schiff, K. (1964). *Abh. Dtsch. Akad. Wiss. Berlin Kl. Chem. Geol. Biol.* **3**, 1–107.
Dowty, E. (2002). *ATOMS*. Version 6.2. Shape Software, 521 Hidden Valley Road, Kingsport, TN 37663, USA.
Ferraris, G. & Gula, A. (2005). *Rev. Mineral. Geochem.* **57**, 69–104.
Ferraris, G., Makovicky, E. & Merlino, S. (2008). *Crystallography of Modular Materials*. Oxford: IUCr/Oxford University Press.
Ferraris, G. & Merlino, S. (2005). Editors. *Micro and Mesoporous Mineral Phases*. Washington, DC: Mineralogical Society of America and Geochemical Society.
Koudsi, U. Y. & Dyer, A. (2001). *J. Radioanal. Nucl. Chem.* **247**, 209–219.
Lin, Z., Rainho, J. P., Rocha, J. & Carlos, L. D. (2006). *Mater. Sci. Forum*, **514–516**, 123–127.
Lin, Z. & Rocha, J. (2004). *Microporous Mesoporous Mater.* **76**, 99–104.
Lin, Z. & Rocha, J. (2005). *Eur. J. Mineral.* **17**, 869–873.
Lin, Z. & Rocha, J. (2006). *Microporous Mesoporous Mater.* **94**, 173–178.
Lin, Z., Rocha, J., Brandão, P., Ferreira, A., Esculcas, A. P. & Pedrosa de Jesus, J. D. (1997). *J. Phys. Chem. B*, **101**, 7114–7120.
Liu, Y., Du, H., Zhou, F. & Pang, W. (1997). *Chem. Commun.* pp. 1467–1468.
McCusker, L. B., Liebau, F. & Engelhardt, G. (2003). *Microporous Mesoporous Mater.* **58**, 3–13.
Merlino, S., Pasero, M., Artioli, G. & Khomyakov, A. P. (1994). *Am. Mineral.* **79**, 1185–1193.
Rocha, J. & Anderson, M. W. (2000). *Eur. J. Inorg. Chem.* pp. 801–818.
Rocha, J. & Lin, Z. (2005). *Rev. Mineral. Geochem.* **57**, 173–201.
Sheldrick, G. M. (2002). *SADABS*. University of Göttingen, Germany.
Sheldrick, G. M. (2008). *Acta Cryst.* A**64**, 112–122.
Sheriff, B. L. & Zhou, B. (2004). *Can. Mineral.* **42**, 1027–1035.
Subbotin, V. V., Merlino, S., Pushcharovsky, D. Yu., Pakhomovsky, Ya. A., Ferro, O., Bogdanova, A. N., Voloshin, A. V., Sorokhtina, N. V. & Zubkova, N. V. (2000). *Am. Mineral.* **85**, 1516–1520.